Electronic Supplementary Material (ESI) for Chemical Communications.

[**Supporting Information**]

Predicting the structure and interfacial activity of diblock brush, mixed brush, and Janus-grafted nanoparticles

Jason Koski,^{a} *Huikuan Chao,*^{a} *and Robert A. Riggleman*^{a*}

[a] Department of Chemical and Biomolecular Engineering, University of Pennsylvania, Philadelphia, PA, USA.; E-mail: rrig@seas.upenn.edu

1 Supplemental Figures

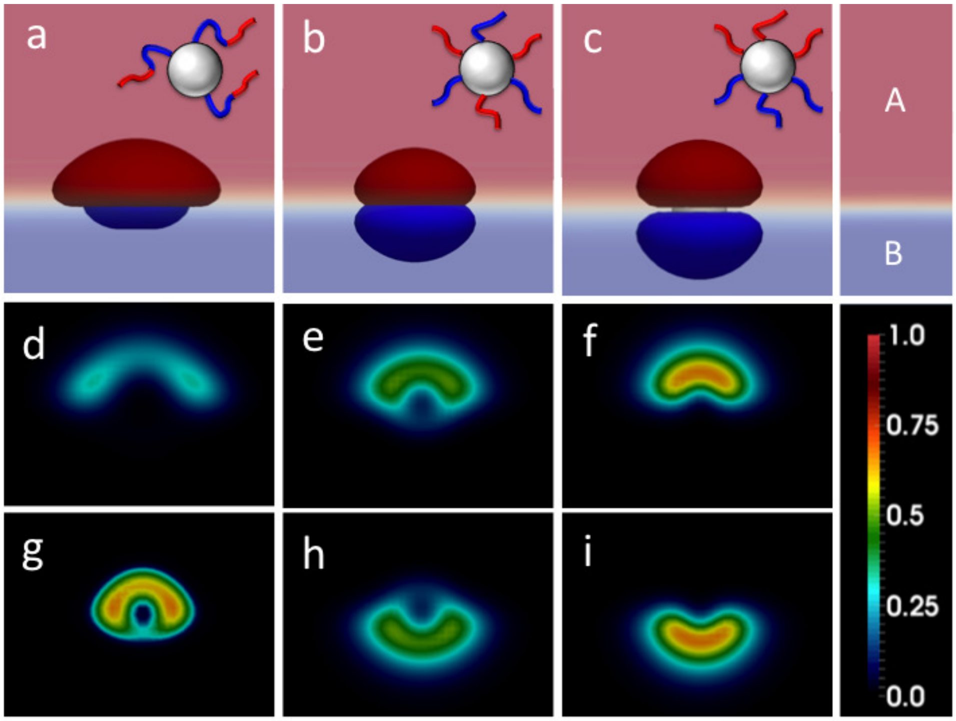

Figure S1: Local grafted chain density for $R_P/R_g = 1$ and $f_A = 0.5$. (a), (d), and (g) display the diblock grafted particles, (b), (e), and (h) display mixed brush particles, while (c), (f), and (i) display the Janus brush particles. (a - c) Isosurfaces of the explicit grafted particle sitting near the interface. The red isosurfaces denote the A grafted monomers while the blue isosurfaces represent the B grafted monomers. The red and blue background show the A and B matrix chain density, respectively. (d - f) Color maps indicating the A grafted chain density. (g - i) Color maps indicating the B grafted chain density. The color maps are taken from slices through the particle center. The color bar denotes the volume fraction of the corresponding component.

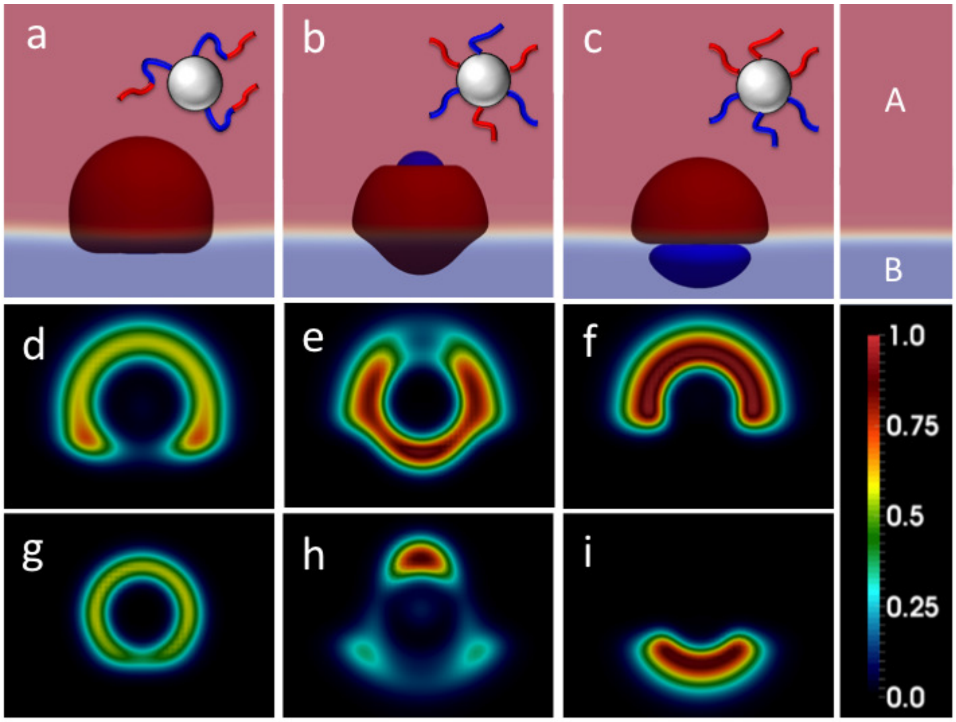

Figure S2: Local grafted chain density for $R_P/R_g = 2.5$ and $f_A = 0.75$. (a), (d), and (g) display the diblock grafted particles, (b), (e), and (h) display mixed brush particles, while (c), (f), and (i) display the Janus brush particles. (a - c) Isosurfaces of the explicit grafted particle sitting near the interface. The red isosurfaces denote the A grafted monomers while the blue isosurfaces represent the B grafted monomers. The red and blue background show the A and B matrix chain density, respectively. (d - f) Color maps indicating the A grafted chain density. (g - i) Color maps indicating the B grafted chain density. The color maps are taken from slices through the particle center. The color bar denotes the volume fraction of the corresponding component.

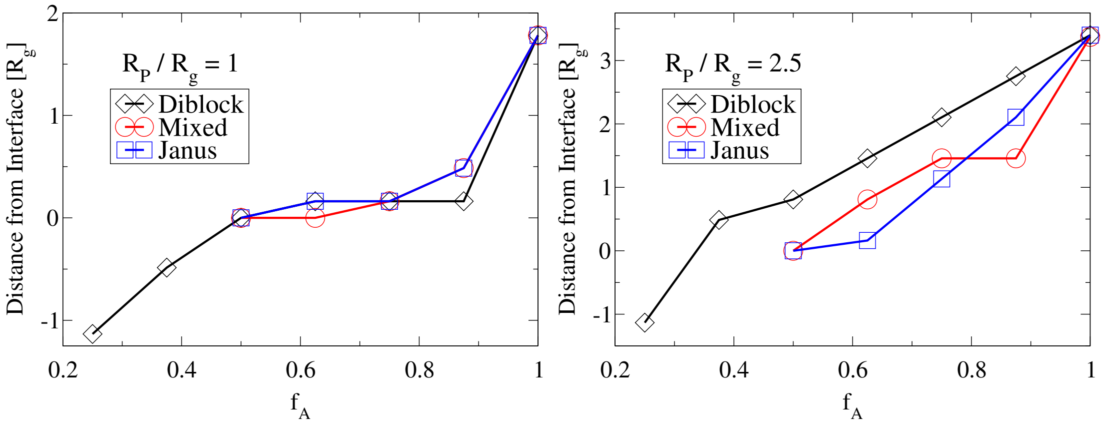

Figure S3: Distance of the explicit particle center to the interface as a function of f_A for $R_P/R_g = 1$ (left) and $R_P/R_g = 2.5$ (right). Negative values correspond to the particle residing predominantly in the B phase while positive values correspond to the particle residing predominantly in the A phase.

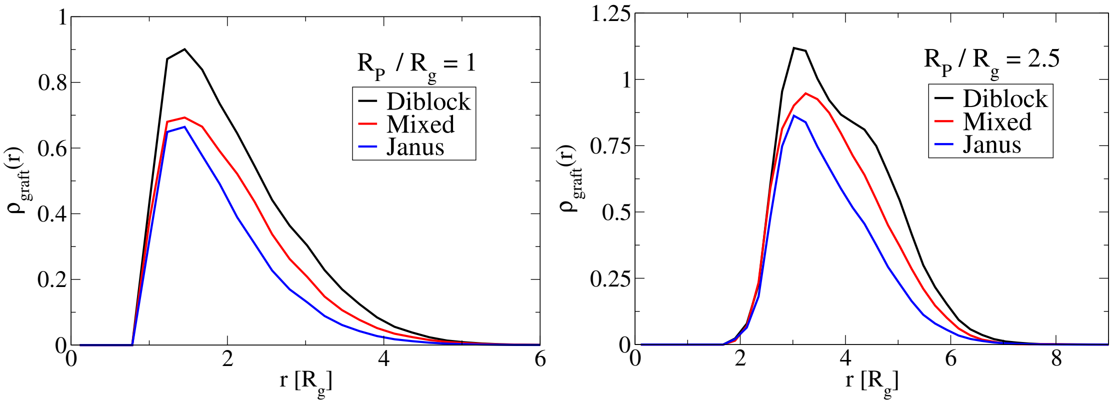

Figure S4: Density of the grafted chains in the plane parallel to the $A-B$ interface versus the distance from the center of the explicit particle for $R_P/R_g = 1$ (left) and $R_P/R_g = 2.5$ (right) at $f_A = 0.5$.

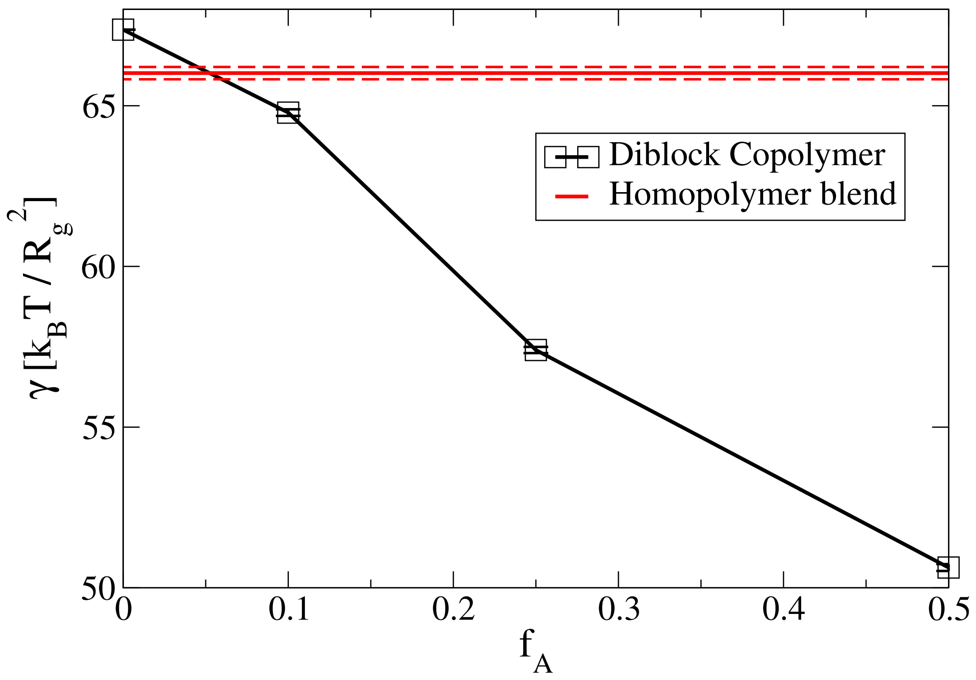

Figure S5: Interfacial tension for pure A/B homopolymer blend and for added diblock as a function of f_A.

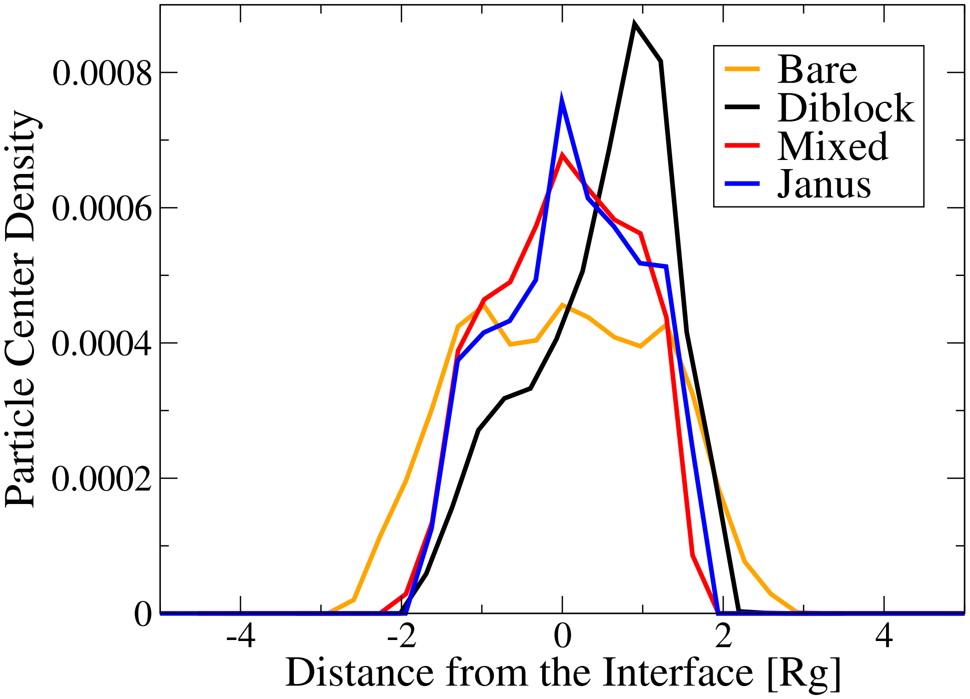

Figure S6: Particle center density versus the perpendicular distance from the interface for $R_P/R_g = 2.5$ at $f_A = 0.5$. Each curve was averaged over three independent complex Langevin trajectories as well as the symmetry of the two A-B interfaces that are in the simulation box. The bare particles sample a wider range of positions relative to the interface, making them less effective at breaking A-B contacts and reducing the interface tension.

2 Theory

The model used in this communication is based on a recent extension of polymer field theory to incorporate polymer nanocomposite systems with grafted nanoparticles.[1] This method enables a pure field theoretic approach for polymer nanocomposite where sampling the fully fluctuating chemical fields is feasible. The current model includes both an A/B homopolymer blend and bare or grafted nanoparticles, where three kinds of grafting (homogenous, mixed, and Janus-grafting) are imposed. The polymers are modeled as discrete Gaussian chains with N interaction sites. The density of a polymer segment is distributed about its center over a unit Gaussian: $h(\mathbf{r}) = (\frac{1}{2\pi b^2})^{3/2}\exp(-\frac{\mathbf{r}^2}{2b^2})$, where b here is the statistical segment length. Thus, the polymer density distribution is defined as

$$\hat{\rho}_K(\mathbf{r}) = (h * \hat{\rho}_{K,c})(\mathbf{r}) \tag{S.1}$$

where $f * g$ is the shorthand notation for the convolution of two functions $f(x)$ and $g(x)$ defined by $(f * g)(x) = \int_{-\infty}^{\infty} dx' f(x - x')g(x')$, and $\hat{\rho}_{K,c}$ is the distribution of polymer segment centers given as:

$$\hat{\rho}_{K,c}(\mathbf{r}) = \sum_{i}^{n_K}\sum_{j}^{N_K} \delta(\mathbf{r} - \mathbf{r}_{i,j}). \tag{S.2}$$

Similar treatment of the density distribution of a single nanoparticle is imposed following our previous works,[1,2] where the distribution of nanoparticle centers for bare and homogenous/mixed grafted nanoparticles is taken as

$$\hat{\rho}_{P,c}(\mathbf{r}) = \sum_{i}^{n_P} \delta(\mathbf{r} - \mathbf{r}_i). \tag{S.3}$$

The Janus-grafted nanoparticles have an orientation associated with them, and the distribution with the additional orientational dependence is given as

$$\hat{\rho}_{P,c}(\mathbf{r}, \mathbf{u}) = \sum_{i}^{n_P} \delta(\mathbf{r} - \mathbf{r}_i)\delta(\mathbf{u} - \mathbf{u}_i). \tag{S.4}$$

To control how the density decays from the bulk segment density, ρ_o in the nanoparticle core to 0 outside, a density distribution function, $\Gamma(\mathbf{r})$ is implemented. For spherical particle, $\Gamma(\mathbf{r})$ has the form:

$$\Gamma(\mathbf{r}) = \frac{\rho_o}{2}\mathrm{erfc}\left(\frac{|\mathbf{r}| - R_P}{\xi}\right), \tag{S.5}$$

where R_P is the nanoparticle radius and ξ is the interfacial width. The interaction between A and B segments has the standard Flory repulsive potential form characterized by χ_{AB} and the local total density in the systems are assumed weakly compressible with a quadratic penalty on the deviations from mean segment density ρ_o given as

$$U = \frac{\kappa}{2\rho_o} \int d\mathbf{r} \left(\sum_i \hat{\rho}_i(\mathbf{r}) - \rho_o \right)^2 , \tag{S.6}$$

where i goes over the matrix, grafted polymer, and the nanoparticle (P) species, and κ controls the incompressibility strength.

The model with the above-mentioned interactions between the segments and the nanoparticles then undergoes a particle-to-field transformation, where the particle-particle interactions are decoupled through Hubbard-Stratonovich transformations[3,4]and replaced with interactions between particles and auxiliary fields. As a result, the model is now a functional of chemical potential fields and no longer a function of the explicit polymer and nanoparticle coordinates. After the transformation, the canonical ensemble partition function becomes a functional integral over a set of chemical fields($[\{w\}]$),

$$\mathcal{Z} = z_o \int \mathcal{D}\{w\} \exp\left(-\mathcal{H}[\{w\}]\right), \tag{S.7}$$

where z_o contains numerical prefactors (e.g. the thermal de Broglie wavelengths), and $\mathcal{H}$ is the effective Hamiltonian.

In the particle-to-field transformation, we can choose to leave a single nanoparticle and its grafted chains out for the sake of calculating the local brush density of the single nanoparticle near the interface. To achieve this, we adopted the hybrid particle-field theory method[5] (HPFT) where a nanoparticle with a fixed orientation and position are described explicitly through a chosen density distribution $\Gamma(\mathbf{r})$. At the same time, grafted chains are grafted onto the explicit nanoparticle surface by following the manner in a previous study.[6] The effective Hamiltonian is now given by

$$\begin{aligned} \mathcal{H}[\mathbf{r}_{EP}; \{w\}] \;=\; & \int d\mathbf{r} \left[\frac{\rho_0}{2\kappa} w_+^2 - i\left(\rho_0 - \hat{\rho}_{EP}\left(\mathbf{r}_{EP}\right)\right)\, w_+ \right] \\ & + \int d\mathbf{r} \left[\frac{\rho_o}{\chi_{AB}} \left([w_{AB}^{(+)}]^2 + [w_{AB}^{(-)}]^2 \right) \right] \\ & - \int d\mathbf{r}_\perp \sigma_{EgA}(\mathbf{r}_\perp) \ln q_{EgA}[\mathbf{r}_\perp; \mu_A] - \int d\mathbf{r}_\perp \sigma_{EgB}(\mathbf{r}_\perp) \ln q_{EgB}[\mathbf{r}_\perp; \mu_B] \\ & - n_A \ln Q_A[\mu_A] - n_B \ln Q_B[\mu_B] - n_P \ln Q_P[\mu_P], \end{aligned} \tag{S.8}$$

where i is the imaginary unit and the terms with the notation E in the subscript are related to the explicit nanoparticle and its grafted chains. For example, $\hat{\rho}_{EP}$ is the explicit particle density distribution and $\mathbf{r}_{EP}$ is the coordinates of the explicit particle. $\sigma_{EgA}(\mathbf{r}_\perp)$ is the distribution of grafting sites at every position $\mathbf{r}_\perp$ on the explicit nanoparticle surface, and q_{EgK} is the partition function of a single K type grafted chain with one end fixed at $\mathbf{r}_\perp$. Each chemical potential field, w, depends on $\mathbf{r}$ but this dependence is suppressed in the above equation for brevity. Lastly, we note that in our sutdy, the partition function does not depend on $\mathbf{r}_{EP}$ because we keep the explicit particle fixed at the center of the box. Here in eqn (S.8), μ_A and μ_B are the chemical fields experienced by the A and B segments defined as

$$\begin{aligned} \mu_A(\mathbf{r}) &= [h * (iw^{(+)} + iw_{AB}^{(+)} - w_{AB}^{(-)})](\mathbf{r}), \\ \mu_B(\mathbf{r}) &= [h * (iw^{(+)} + iw_{AB}^{(+)} + w_{AB}^{(-)})](\mathbf{r}). \end{aligned} \tag{S.9}$$

The molecular partition function, Q_K, for the K type matrix homopolymer is obtained by first calculating the chain propagator $q_K(\mathbf{r}, j)$, where the dependence on μ_K is dropped for the sake of simplicity. The chain propagator can be obtained by iterating the corresponding Chapman-Kolmogorov equation

$$q_K(\mathbf{r}, j) = e^{-\mu_K(\mathbf{r})} \int d\mathbf{r}' \ \Phi(|\mathbf{r} - \mathbf{r}'|) \, q_K(\mathbf{r}', j-1), \tag{S.10}$$

where $\Phi(\mathbf{r}) = (\frac{3}{2\pi b^2})^{3/2} \exp(-\frac{3\mathbf{r}^2}{2b^2})$ is the normalized bond transition probability and the initial condition at $j = 1$ has the form $q_K(\mathbf{r}, j = 1) = \exp[-\mu_K(\mathbf{r})]$. Then Q_K is in turn obtained as

$$Q_K = \frac{1}{V} \int d\mathbf{r} q_K(\mathbf{r}, P). \tag{S.11}$$

After obtaining both q_K and Q_K, the matrix homopolymer segment center density operator is given as[4]

$$\tilde{\rho}_K(\mathbf{r}) = \frac{n_K}{VQ_K} \sum_{j=1}^{P} q_K(\mathbf{r}, j) \, e^{\mu_K(\mathbf{r})} \, q_K(\mathbf{r}, P - j), \tag{S.12}$$

and the distribution of the total segment mass is then defined as

$$\breve{\rho}_K(\mathbf{r}) = (h * \tilde{\rho}_K)(\mathbf{r}). \tag{S.13}$$

The chemical potential field μ_P that is conjugate with the grafted nanoparticle centers has different forms depending on the architecture of grafted chains and the distribution of grafting sites. For the case of the homogenously grafted $A - B$ diblock copolymer, μ_P has the form

$$\mu_{P,diblock}(\mathbf{r}) = (\Gamma * iw_+)(\mathbf{r}) - \frac{n_{gD}}{n_P} \left(\Gamma_\sigma * \ln q_{gD}\right)(\mathbf{r}), \tag{S.14}$$

where n_{gD} is the total number of grafted $A - B$ diblock copolymer chains in the system and $q_{gD}(\mathbf{r})$ is the partition function of single grafted $A - B$ diblock copolymer and $\Gamma_\sigma(\mathbf{r})$ imposes the homogenous distribution of grafting sites. The first term in eqn (S.14) accounts for the penalty from density overlap between the neutral particle core and the other components, and remains the same regardless of the distribution of grafting sites. The grafting sites are $Rp + \xi$ away from the nanoparticle center with a thickness controlled by ξ,

$$\Gamma_\sigma(\mathbf{r}) = \frac{1}{\sigma_0} \exp\left[-\left(\frac{|\mathbf{r}| - R_P - \xi}{\xi} \right)^2 \right], \tag{S.15}$$

where σ_0 in the prefactor normalizes Γ_σ such that $\int d\mathbf{r}\Gamma_\sigma(\mathbf{r}) = 1$. Therefore the total normalized distribution of grafting sites can be defined as the convolution between Γ_σ and the nanoparticle center distribution $\rho_{P,c}(\mathbf{r})$,

$$\sigma_g(\mathbf{r}) = \frac{1}{n_P}\left(\Gamma_\sigma * \rho_{P,c}\right)(\mathbf{r}). \tag{S.16}$$

The second term in eqn (S.14) varies when an A/B mixed homopolymer brush is grafted as follows:

$$\begin{aligned} \mu_{P,mixed}(\mathbf{r}) &= (\Gamma * iw_+)(\mathbf{r}) \\ &\quad -\frac{n_g}{n_P}\left[\Gamma_\sigma * \left(f_A \ln q_{gA} + (1-f_A)\ln q_{gB}\right)\right](\mathbf{r}), \end{aligned} \tag{S.17}$$

where f_A is the overall volume fraction of the grafted chains that is component A and n_g is the total number of grafted chains. The normalized distribution of grafting sites for both A and B grafted chains have the same form and given as

$$\sigma_{gA}(\mathbf{r}) = \sigma_{gB}(\mathbf{r}) = \frac{1}{n_P}\left(\Gamma_\sigma * \rho_{P,c}\right)(\mathbf{r}). \tag{S.18}$$

For the case of Janus grafting, μ_P needs to be reconstructed and the final result has the form given as

$$\begin{aligned} \mu_{P,Janus}(\mathbf{r},\mathbf{u}) &= (\Gamma * iw_+)(\mathbf{r}) - \frac{n_g}{n_P}\Bigg[f_A(\tilde{\Gamma}_{\sigma A} * \ln q_{gA})(\mathbf{r},\mathbf{u}) \\ &\quad +(1-f_A)(\tilde{\Gamma}_{\sigma B} * \ln q_{gB})(\mathbf{r},\mathbf{u})\Bigg], \end{aligned} \tag{S.19}$$

where $\tilde{\Gamma}_{\sigma A}(\mathbf{r},\mathbf{u})$ and $\tilde{\Gamma}_{\sigma B}(\mathbf{r},\mathbf{u})$ are the symmetrical functions of the distributions of Janus grafting sites, $\Gamma_{\sigma A}(\mathbf{r},\mathbf{u})$ and $\Gamma_{\sigma B}(\mathbf{r},\mathbf{u})$, about the origin and have the relationship, $\tilde{\Gamma}_{\sigma K}(\mathbf{r},\mathbf{u}) = \Gamma_{\sigma K}(-\mathbf{r},\mathbf{u})$. The detailed description of eqn (S.19) follows in section 3. According to the inclusion of orientation dependence in $\Gamma_{\sigma K}$, σ_{gK} is in turn redefined to integrate over the orientation space as follows:

$$\sigma_{gK}(\mathbf{r}) = \int d\mathbf{u}\ (\rho_{P,c} * \Gamma_{\sigma K})(\mathbf{r},\mathbf{u}). \tag{S.20}$$

The definitions of $\Gamma_{\sigma K}$ and $\tilde{\Gamma}_{\sigma K}$ functions and the derivation for μ_p in the Janus grafting case are included in the following section.

Then, the partition function of a single nanoparticle has the form

$$Q_{P,Janus} = \frac{1}{4\pi V}\int d\mathbf{r}\int d\mathbf{u}\exp\left[-\mu_{P,Janus}(\mathbf{r},\mathbf{u})\right], \tag{S.21}$$

The nanoparticle center density operator is now dependant on both $\mathbf{r}$ and $\mathbf{u}$ and is constructed by

$$\breve{\rho}_{P,c}(\mathbf{r},\mathbf{u}) = \frac{n_P \exp[-\mu_{P,Janus}(\mathbf{r},\mathbf{u})]}{4\pi V Q_P}, \tag{S.22}$$

The total nanoparticle density is given as a integral of the convolution between $\breve{\rho}_{P,c}$ and Γ

$$\breve{\rho}_P(\mathbf{r}) = \int d\mathbf{u}\ (\breve{\rho}_{P,c} * \Gamma)(\mathbf{r},\mathbf{u}). \tag{S.23}$$

The total distribution of grafting sites is also given as a integral of a similar convolution,

$$\breve{\sigma}_{gK}(\mathbf{r}) = \int d\mathbf{u}\ (\breve{\rho}_{P,c} * \Gamma_{\sigma K})(\mathbf{r},\mathbf{u}). \tag{S.24}$$

After the construction of $\breve{\sigma}_{gK}$, the grafted chain segment center density operator can be calculated in a similar manner as in eqn (S.12)

$$\tilde{\rho}_{gK}(\mathbf{r}) = \sum_{j=1}^{N} q_{gK}(\mathbf{r},j)\, e^{\mu_K(\mathbf{r})}\, q^{\dagger}_{gK}(\mathbf{r},N-j), \tag{S.25}$$

where q_{gK} and $q^{\dagger}_{gK}$ are the grafted chain propagators from the free end and the grafted end, respectively. The initial conditions for the two propagators used in solving the corresponding Chapman-Kolmogorov equations are given as

$$\begin{aligned} q_{gK}(\mathbf{r},0) &= \exp[-\mu_K(\mathbf{r})], & \text{(S.26)} \\ q^{\dagger}_{gK}(\mathbf{r},0) &= \frac{\breve{\sigma}_{gK}(\mathbf{r})}{q_{gK}(\mathbf{r},N)} \exp[-\mu_K(\mathbf{r})]. & \text{(S.27)} \end{aligned}$$

3 Janus Grafted Nanoparticle

For the case of Janus grafted particles, each particle is given an unit orientation vector, $\mathbf{u}$, so that the nanoparticles can rotate and the grafting sites for the A and B chains can properly be defined based on the particle's preferred orientation. Here we provide the key steps of the derivation of the orientation-dependent chemical potential field, $\mu_{P,Janus}(\mathbf{r},\mathbf{u})$.

For a Janus grafted nanoparticle, Γ_σ for A and B type grafted chains is taken as

$$\begin{aligned} \Gamma_{\sigma A}(\mathbf{r},\mathbf{u}) &= \frac{1}{\sigma_0} \exp\left[-\left(\frac{|\mathbf{r}| - R_P - \xi}{\xi}\right)^2\right] & \text{(S.28)} \\ &\quad \operatorname{erfc}\left(\frac{1 - 2f_A - \mathbf{r}\cdot\mathbf{u}/|\mathbf{r}|}{\xi_{\mathbf{u}}}\right), \\ \Gamma_{\sigma B}(\mathbf{r},\mathbf{u}) &= \frac{1}{\sigma_0} \exp\left[-\left(\frac{|\mathbf{r}| - R_P - \xi}{\xi}\right)^2\right] \\ &\quad \operatorname{erfc}\left(\frac{\mathbf{r}\cdot\mathbf{u}/|\mathbf{r}| - 1 + 2f_A}{\xi_{\mathbf{u}}}\right), \end{aligned}$$

where the second term in each distribution confines the grafting sites to an area, which consists of a fraction of the total nanoparticle surface area valued at f_A and $1 - f_A$ for A and B type grafted chains, respectively. Here, $\xi_{\mathbf{u}}$ is the boundary width of the confined areas, and the orientation $\mathbf{u}$ is a unit vector pinned at the nanoparticle center and pointing to the center of the A type chain grafting area. From a geometric point of view, $1-2f_A$ in the second term gives the cosine of the angle between $\mathbf{u}$ and the grafting area boundary, while $\mathbf{r} \cdot \mathbf{u}/|\mathbf{r}|$ gives the cosine of the angle between $\mathbf{r}$ and $\mathbf{u}$. Thus, the second term in $\Gamma_{\sigma K}$ controls how the grafting density decays from the bulk value in the corresponding grafting area to 0 in cosine space (Figure S7).

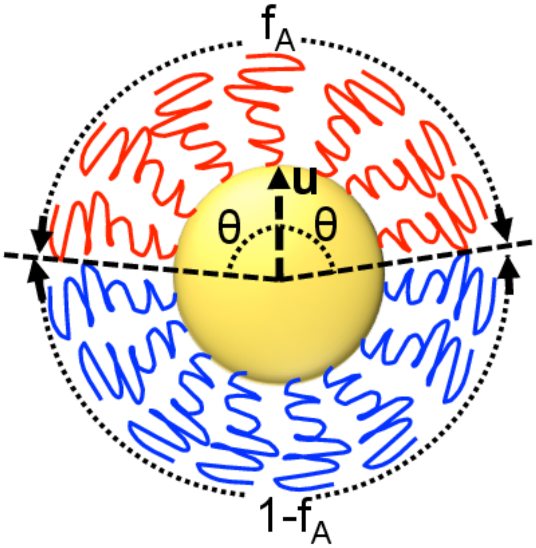

Figure S7: Schematic for the Janus grafted nanoparticle showing the setup for the orientation $\mathbf{u}$, the fraction of grafting area for each type of chain, and the angle θ between $\mathbf{u}$ and the directions long the grafting area boundaries (dashed lines), which has the value at $\theta = \cos^{-1}(1 - 2f_A)$

Next, in order to derive the chemical field conjugate with the Janus grafted nanoparticle, we need to start the deviation from the system's partition function from the step after the particle-to-field transformation where the dependence on the coordinates of matrix polymers has been integrated out, leaving the explicit dependence on the coordinates of the grafted chains and the nanoparticles

$$\begin{aligned} \mathcal{Z} &= z_0 \int \mathcal{D}\{w\} \int d\mathbf{r}^{n_P} \int d\mathbf{u}^{n_P} \int d\mathbf{r}^{n_{gA}N} \exp\Bigg[- \mathcal{H}_{w_\pm,Q} \\ &\quad -i \int d\mathbf{r}\; [\Gamma * w_+](\mathbf{r})\; \hat{\rho}_{P,c}(\mathbf{r}) \\ &\quad - \int d\mathbf{r}\; \mu_A(\mathbf{r})\; \hat{\rho}_{gA,c}(\mathbf{r}) \Bigg], \end{aligned} \tag{S.29}$$

where $\mathcal{H}_{w_\pm,Q}$ consists of the first two integrals in eqn (S.8) plus $n_A \ln Q_A$ and $n_B \ln Q_B$. To keep our derivation concise, in eqn (S.29) we only kept the terms associated with A type grafted chains but dropped the terms associated with the explicit particles and B type grafted chains, the latter of which could be treated in a similar manner. Following the Appendix in our previous work[1] and using eqn (S.20) , the coordinates of grafted chains are integrated out giving rise to the partition function of single grafted chain, $q_{gA}(\mathbf{r}_g)$. The last term in eqn (S.29) can then be rewritten to show the explicit dependence on the nanoparticle coordinates as the follows,

$$\begin{aligned}\mathcal{Z} \;=\; & z_0 \int \mathcal{D}\{w\} \int d\mathbf{r}^{n_P} \int d\mathbf{u}^{n_P} \exp\Bigg[-\mathcal{H}_{w_\pm,Q} \\ & -i\int d\mathbf{r}\; [\Gamma * w_+](\mathbf{r})\; \hat{\rho}_{P,c}(\mathbf{r}) \\ & +n_{gA} \int d\mathbf{u} \int d\mathbf{r}_g \int d\mathbf{r}' \Gamma_{\sigma A}(\mathbf{r}_g - \mathbf{r}', \mathbf{u}) \\ & \hat{\rho}_{P,c}(\mathbf{r}', \mathbf{u}) \ln q_{gA}(\mathbf{r}_g) \Bigg]. \end{aligned} \tag{S.30}$$

where the integral over r_g covers the distribution of all grafting sites in the system. Since Γ_σ is not an even function about $\mathbf{r}$, we change $\tilde{\Gamma}_{\sigma A}(\mathbf{r}, \mathbf{u})$ for $\Gamma_{\sigma A}(-\mathbf{r}, \mathbf{u})$ here and obtain a new convolution between $\tilde{\Gamma}_\sigma$ and $\ln q_{gA}$. After rearranging the order of the integrals,

$$\begin{aligned}\mathcal{Z} \;=\; & z_0 \int \mathcal{D}\{w\} \int d\mathbf{r}^{n_P} \int d\mathbf{u}^{n_P} \exp\Bigg[-\mathcal{H}_{w_\pm,Q} \\ & -i\int d\mathbf{r}\; [\Gamma * w_+](\mathbf{r})\; \hat{\rho}_{P,c}(\mathbf{r}) \\ & +n_{gA} \int d\mathbf{u} \int d\mathbf{r}' \hat{\rho}_{P,c}(\mathbf{r}', \mathbf{u}) (\tilde{\Gamma}_{\sigma A} * \ln q_{gA})(\mathbf{r}', \mathbf{u}) \Bigg]. \end{aligned} \tag{S.31}$$

Now, $\hat{\rho}_{P,c}$ in the last two terms can be combined leading to the $\mu_{P,Janus}$ as in eqn (S.19). Finally, $\hat{\rho}_{P,c}$ can be integrated out in the partition function giving rise to eqn (S.8).

4 Numerical Methods

The fluctuating chemical fields in our field theoretic model are complex valued, which leads to the non-positive definite nature of the effective Hamiltonian. This issue precludes the usage of Monte Carlo method to sample the fluctuating fields. To circumvent the problem, we adopt the complex Langevin (CL) method,[4,7–9] which has been demonstrated capable of efficiently sampling the complex-valued fluctuating fields and evaluating the functional integrals in eqn (S.7) that extend over the entire complex plane.[1,2,10–13] In the CL method, the fields are updated according to the following scheme

$$\frac{\partial w(\mathbf{r})}{\partial t} = -\lambda \frac{\delta H}{\delta w(\mathbf{r})} + \eta(\mathbf{r}, t), \tag{S.32}$$

where t is the pseudo evolution time and η is a real Gaussian white noise with the statistics

$$
\begin{aligned}
< \eta(\mathbf{r}, t) > &= 0, && \text{(S.33)} \\
< \eta(\mathbf{r}, t)\eta(\mathbf{r}', t') > &= 2\lambda\delta(t - t')\delta(\mathbf{r} - \mathbf{r}'). && \text{(S.34)}
\end{aligned}
$$

It is noted that when the noise term in the CL scheme is dropped, the fields evolve according to the mean-field approximations which becomes exact as the chain density $C \to \infty$. The functional derivatives in the CL scheme for each chemical field are listed below

$$
\begin{aligned}
\frac{\delta H}{\delta w_+(\mathbf{r})} &= \frac{\rho_o}{\kappa} w_+(\mathbf{r}) - i\rho_o + i\Bigg[\breve{\rho}_A(\mathbf{r}) && \text{(S.35)} \\
&\quad + \breve{\rho}_{gA}(\mathbf{r}) + \breve{\rho}_B(\mathbf{r}) + \breve{\rho}_{gB}(\mathbf{r}) + \tilde{\rho}_P(\mathbf{r})\Bigg],
\end{aligned}
$$

$$
\begin{aligned}
\frac{\delta H}{\delta w_{AB}^{(+)}} &= \frac{2\rho_o}{\chi_{AB}} w_{AB}^{(+)} + i\Bigg[\breve{\rho}_A(\mathbf{r}) && \text{(S.36)} \\
&\quad + \breve{\rho}_{gA}(\mathbf{r}) + \breve{\rho}_B(\mathbf{r}) + \breve{\rho}_{gB}(\mathbf{r})\Bigg],
\end{aligned}
$$

$$
\begin{aligned}
\frac{\delta H}{\delta w_{AB}^{(-)}} &= \frac{2\rho_o}{\chi_{AB}} w_{AB}^{(-)} - \breve{\rho}_A(\mathbf{r}) && \text{(S.37)} \\
&\quad - \breve{\rho}_{gA}(\mathbf{r}) + \breve{\rho}_B(\mathbf{r}) + \breve{\rho}_{gB}(\mathbf{r}).
\end{aligned}
$$

A predictor-corrector scheme[12] was used to evolve the fields according to the CL method in eqn (S.32) with the step size $\lambda\Delta t = 5 \times 10^{-5}$ in all the CL simulations. All the density distribution quantities are obtained from averaging the results over 5,000 iterations after equilibration sampled every 50 iterations. The orientation $\mathbf{u}$ in the unit sphere are discretized under the spherical coordinates by choosing $N_{\mathbf{u}} = 12$ polar angles and $2N_{\mathbf{u}} = 24$ azimuthal angles. The integrals over angles are determined according to the Gaussian-Legendre quadrature rule.

For the dimension of the 3D simulation boxes, the length of the box in the $z-$direction is fixed at $L_z = 34R_g$ across all simulations. The x and $y-$directions for systems with $R_P/R_g = 1.0$ have sizes valued at $L_x = L_y = 15.87R_g$ in the HPFT simulations and $L_x = L_y = 6.8R_g$ in fully field theoretic simulations. In systems with $R_P/R_g = 2.5$, L_x and L_y have values of $26.22R_g$ and $20.4R_g$ in the HPFT simulation with and without implicit nanoparticle neighbors, respectively, and in the fully field theoretic simulations $L_x = L_y = 11.33R_g$.

Other numerical parameter includes the spacial resolution dx fixed at $dx = 0.33R_g$, the interfacial width of the nanoparticle density distribution $\xi = 0.17R_g$, and the boundary width of the Janus grafting area $\xi_{\mathbf{u}} = 0.13$.

References

[1] H. Chao, B. A. Hagberg and R. A. Riggleman, *Soft Matter*, 2014, **10**, 8083–8094.

[2] J. Koski, H. Chao and R. A. Riggleman, *The Journal of Chemical Physics*, 2013, **139**, 244911.

[3] P. M. Chaikin and T. C. Lubensky, *Principles of Condensed Matter Physics*, Cambridge Univ Press, 2000, vol. 1.

[4] G. H. Fredrickson, *The Equilibrium Theory of Inhomogeneous Polymers*, Oxford University Press, New York, 2006.

[5] S. Sides, B. Kim, E. Kramer and G. Fredrickson, *Physcial Review Letters*, 2006, **96**, 250601.

[6] J. U. Kim and M. W. Matsen, *Physial Review Letters*, 2009, **102**, 78303.

[7] G. H. Fredrickson, V. Ganesan and F. Drolet, *Macromolecules*, 2002, **35**, 16–39.

[8] G. Parisi, *Physics Letters B*, 1983, **131**, 393–395.

[9] J. Klauder, *Physical Review A*, 1984, **29**, 2036–2047.

[10] R. A. Riggleman, R. Kumar and G. H. Fredrickson, *The Journal of Chemical Physics*, 2012, **136**, 024903.

[11] R. A. Riggleman and G. H. Fredrickson, *The Journal of Chemical Physics*, 2010, **132**, 024104.

[12] D. J. Audus, K. T. Delaney, H. D. Ceniceros and G. H. Fredrickson, *Macromolecules*, 2013, **46**, 8383–8391.

[13] M. C. Villet and G. H. Fredrickson, *The Journal of Chemical Physics*, 2010, **132**, 034109.